A study of local heating of molecules under Surface Enhanced Raman Scattering (SERS) conditions using the anti-Stokes/Stokes ratio

R. C. Maher,*[a] L. F. Cohen,[a] E. C. Le Ru[b] and P. G. Etchegoin*[b]

Received 20th July 2005, Accepted 25th July 2005
First published as an Advance Article on the web 18th October 2005
DOI: 10.1039/b510413k

We make systematic measurements of the anti-Stokes/Stokes (aS/S) ratios using low power lasers (0.5 mW at 514 and 633 nm) of rhodamine 6G (RH6G) on dried silver colloids over a wide range of temperatures from 140 to 350 K. We show that a scan in temperature allows the extraction of the contributions to the anti-Stokes/Stokes ratio from resonance effects and heating independently, thus decoupling the two aspects of the problem.

1. Introduction

Surface Enhanced Raman spectroscopy (SERS)[1,2] continues to attract interest. Currently SERS is being proposed as a method for genetic screening,[3,4] health diagnostics,[5] intracellular imaging[6] and therapeutic methods for cancer detection and treatment. A full comprehension of the interactions between analyte and nanostructured SERS metallic surface is therefore essential if these possibilities are to be realized as useful techniques. An important issue is if the huge local electromagnetic (EM) fields cause heating even at relatively low power, as this may damage tissue under study in some cases or may reveal in other cases interesting aspects of the SERS problem such as vibrational pumping. Under certain circumstances plasmon-related heating effects may even be desirable[7] for biomedical applications. Nevertheless, the magnitude of the effect and how to control it needs yet to be characterized. In addition, robust methods to determine the SERS enhancements are still not established.

The measurement of the anti-Stokes/Stokes ratio as a function of laser power was put forward as a potential metrology solution to establish Raman cross sections under the conditions that SERS pumping could be created.[8] Over a series of previous papers we have looked at this problem in some detail. Firstly, we studied the anti-Stokes/Stokes ratio as a function of laser power and laser frequency and demonstrated evidence for an imbalance in population which can be related to pumping under certain conditions[9] or selective vibrational heating. The anomalous ratio that is commonly measured even at low power was predicted to relate to hidden resonances in the system[10,11] and we have recently demonstrated that this is indeed the case.[12] In addition, the question of whether power dependent changes to the SERS signal are only related to heating,[10] rather than pumping, have been re-examined using alternative methods to anti-Stokes/Stokes ratios.[13] The ratios can, in general, be influenced by various factors making the interpretation complex. The main contributing factors to the aS/S ratios include heating, pumping, and resonance effects.

In this paper we focus our attention on evidence for heating even at low power under SERS conditions using measurements of the aS/S ratio of Rhodamine 6G (RH6G) over a broad range of temperatures from 140 to 350 K. Measurements have been made at laser frequencies both away

[a] *The Blackett Laboratory, Imperial College London, Prince Consort Road, London, UK, SW7 2BW. E-mail: Robert.Maher@imperial.ac.uk*
[b] *The MacDiarmid Institute for Advanced Materials and Nanotechnology, School of Chemical and Physical Sciences, Victoria University of Wellington, P.O. Box 600, Wellington, New Zealand. E-mail: Pablo.Etchegoin@vuw.ac.nz*

from and close to the main absorption peak of the dye. We find evidence for a temperature rise at low laser power ≈ 0.5 mW that depends on laser frequency. Above all, we find that by performing a temperature scan the relative contributions of direct heating and underlying resonances affecting the cross section at the Stokes and anti-Stokes frequencies can be decoupled to a large extent.

1.1. Heating and pumping definitions

For the sake of clarity, we first set out our definitions of the various heating scenarios that can occur under SERS conditions.[13] In the following T_{env} is the temperature of the local environment where the environment includes the supporting substrate and the air surrounding the colloid and analyte, T_{room} is room temperature. T_{met} is the temperature of the metal colloids and T_{mol} is the temperature of the molecule. The main scenarios are:

- For a sufficiently low laser power the whole system is in thermal equilibrium and there is no heating. In this case $T_{room} = T_{env} = T_{met} = T_{mol}$.
- Global heating is when the system remains in thermal equilibrium at a temperature higher than room temperature $T_{env} = T_{met} = T_{mol}$ and all of them $> T_{room}$.
- Non-equilibrium heating occurs when $T_{met} = T_{mol} \geq T_{room} \geq T_{env}$. As the molecules are directly adsorbed onto the surface of the colloids they interact strongly with them and can be assumed to be in thermal equilibrium with the metal.

There are also more exotic effects related to vibrational pumping of the molecule as a whole, or even pumping of specific modes, but whether these present themselves as enhancement of the cross-section or a direct temperature rise is still a point of discussion.

1.2. Resonances

The interpretation of the SERS anti-Stokes/Stokes ratio can be complicated by the introduction of many possible sources of resonance. The most general expression for the ratio under SERS conditions at low power (in the absence of pumping and for molecules in thermal equilibrium at temperature T) is:[14,15]

$$\rho = \frac{I_{AS}}{I_S} \propto \frac{(\omega_L + \omega_v)^4}{(\omega_L - \omega_v)^4} \exp(-\hbar\omega_v / k_B T) \frac{\sigma_{AS}}{\sigma_S} \sum_{i=1}^{N} \frac{A_{AS}^2}{A_S^2} \quad (1)$$

where $I_{AS(S)}$ is the intensity of the anti-Stokes (Stokes) Raman mode, $\omega_{L(v)}$ is the frequency of the laser (Raman mode), T is the temperature of the sample, $\sigma_{AS(S)}$ is the anti-Stokes (Stokes) scattering cross section of the molecule adsorbed to the surface, N is the number of active molecules (not necessarily all molecules in the probe volume), and $A_{AS(S)}$ is the enhancement of the local field at the molecule at the anti-Stokes (Stokes) frequency. The latter term includes both electromagnetic and chemical enhancement effects. In general the enhancement can be site dependent and therefore should be summed over all active sites.

As we will show in the following, by investigating how this ratio changes as a function of temperature over a wide temperature range, we can separate the contributions due to heating and resonance effects. This remarkable fact will be the main objective and conclusion of this paper.

2. Experimental

Silver colloids were produced by reduction of $AgNO_3$ with sodium citrate (all chemicals purchased from Sigma except where stated), using the procedure described by Lee and Meisel.[16] The colloids produced from this technique have a distribution of sizes with a mean diameter of 60 nm as revealed by dynamic light scattering (DLS) in solution and scanning electron microscopy (SEM) on dry samples. The resulting colloidal suspension is brown–yellow in appearance and is stable for several months at 4–5 °C.

SERS active samples were prepared by mixing equal amounts of colloidal and 25 mM KCl solutions together to which 1 μl of 10^{-6} M Rhodamine 6G (RH6G) solution was added. The resulting solution was of 10^{-9} M RH6G concentration, a small amount of which was then dried onto a silicon substrate.

SERS experiments were carried out using a Renishaw 2000 CCD spectrometer equipped with an Olympus BH-2 confocal microscope and a Linkham temperature control stage. Measurements were taken using both 514 nm Ar^+ ion and 633 nm HeNe lasers. Light was focused onto the sample surface using a $\times 50$ long working distance objective for all measurements. This objective produced a beam width of approximately 1.5 μm in diameter at the focal point. Intensities within 250 cm^{-1} of the laser were distorted by the notch filter rendering peaks within this region unusable for the determination of anti-Stokes/Stokes ratios. Laser power was fixed at 0.5 mW. The temperature of the sample was varied between 100 K and 370 K in 10 K intervals.

Raman data was taken with integration times of between 1 and 30 s depending on the specific sample. Five or more measurements were made in different locations on the sample to gain an average over the various scattering geometries. The Raman peaks were then analyzed using standard Voigt functions with subtracted backgrounds (Peakfit and Origin).

It is of critical importance for these measurements that the temperature of the sample and system response are precisely calibrated. The system's optical response was calibrated using the Raman spectrum of paracetamol which is shown as an inset (a) of Fig. 1. This compound has a large number of strong Raman modes over the range we are interested in. It also has a maximum absorption far from either of the two lasers we used (at approximately 250 nm) thus minimizing the effect of resonances with the molecule itself. The aS/S ratio (ρ) was calculated for all visible peaks and these were compared to the theoretical values for both lasers. This allowed us to obtain calibration curves which were then used to correct the SERS measurements. This corrects for any possible spectral artifacts arising from the collecting optics, notch filter, grating, or CCD in the reported values. Fig. 1 shows that there is good agreement between the experimental and the theoretical ratio determined from eqn. (1) with the asymmetry term (to be defined later in eqn. (2))

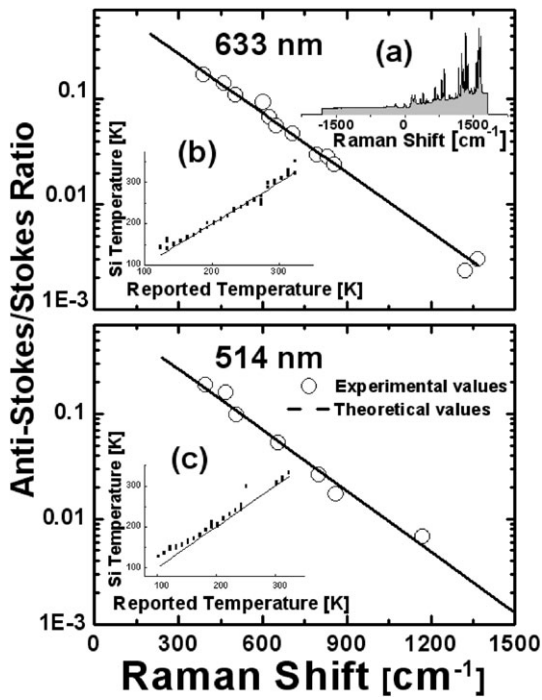

Fig. 1 Anti-Stokes/Stokes ratios of Raman active paracetamol modes for the 633 nm and 514 nm lasers. These agree well with the theoretical ratio (dashed lines) determined using eqn. (1) with the enhancement set to unity. Inset (a) shows the full Raman spectrum of paracetamol. Insets (b) and (c) show the sample temperature as calculated using the ratio of the 520 cm^{-1} mode of silicon for the 633 and 514, respectively, against the temperature reported by the thermostat. The lines on these insets represents the temperature reported by the thermostat.

set to one and assuming that there was no local heating due to the laser under normal Raman conditions.

The temperature of the sample surface was determined by performing a Raman measurement on the silicon substrate in close proximity to each of the SERS measurement locations. This removed any artifacts arising from the thermal contact between the sample and the cold finger. The aS/S ratio of silicon's 520 cm^{-1} peak were corrected using the same factors applied to the paracetamol case above. Eqn. (1) was then used to determine the sample's temperature for each SERS measurement. Insets (b) and (c) of Fig. 1 show the temperature determined from silicon plotted against the temperature reported from the thermostat. The two completely independent uses of the same correction factors (for paracetamol and Si) support their validity.

Once the RH6G data had been taken, the variation in the aS/S for each mode was fitted according to:

$$\rho = A\frac{(\omega_L + \omega_v)^4}{(\omega_L - \omega_v)^4}\exp(-\hbar\omega_v/k_B(T_{Si} + \Delta T_{mode})) \quad (2)$$

where A is the asymmetry factor measuring contributions from resonance effects (asymmetries in cross section) and ΔT_{mode} is the temperature rise above the silicon substrate. The parameter A in eqn. (2) will depend on the particular phonon under consideration and accounts for any asymmetry in the cross section from the anti-Stokes to the Stokes side which is not accounted for under normal scattering conditions. Since SERS takes place under a background of (plasmon) resonances, it is not expected in general for the cross section of a vibration at the anti-Stokes frequency to be exactly the same as the cross section on the Stokes side; this is the physical origin of the asymmetry parameter A. We call the situation represented by eqn. (2) the $(A + \Delta T)$ fit. Fits were also performed by setting $A = 1$ or $\Delta T_{mode} = 0$ in eqn. (2) and these are referred to as the ΔT only and A only fits, respectively. Additionally, we have also fitted some data using a model where the ΔT is an independent variable shared between the data sets whilst the A is varied independently for each. We call this $A + \Delta T$ shared. The assumption that ΔT will be independent of T itself can be justified to a large extent by the almost constant value of the specific heat of solids (Ag in particular) in the temperature range where we perform the experiments. But the validity of this assumption has to be evaluated ultimately by judging the quality of the fits to reproduce the measured data. We found that this assumption holds very well in reproducing the experimental values as shown in the next section.

3. Results

We first present data using the 633 nm laser. Figs. 2 and 3 show examples of anti-Stokes/Stokes ratio values as a function of temperature for two modes, the 610 and 1510 cm^{-1} modes of RH6G, respectively. A wider range of temperatures can be accessed using the 610 cm^{-1} mode because unlike the higher modes it is more heavily populated being at a lower energy on the anti-Stokes side. For both figures we show the theoretically predicted behavior ($A = 1$, $\Delta T = 0$) and the fits to experimental data using the $(A + \Delta T)$, A only, and ΔT only models. Note that the low populations of the higher modes also causes the anti-Stokes of these modes to be less well defined resulting in a greater scatter in the results obtained.

The experimental data for the 610 cm^{-1} mode is best approximated by the $(A + \Delta T)$ fit. However, the ΔT only fit does come close to approximating the data whilst the A only is the worst fit of the three models. In the case of the 1510 cm^{-1} mode the data is again best approximated by the $(A + \Delta T)$ fit. We found that this was the case for the other modes investigated. The fitting to all the modes is summarized in Table 1, including the $A + \Delta T$ shared model.

Fig. 4 shows the equivalent data for the 610 cm^{-1} mode when the sample is illuminated with the 514 nm laser. The peaks associated with the higher modes were too small, particularly on the anti-Stokes side, for the 514 nm laser at these laser powers. There are significant differences in the extracted A and ΔT values. The $(A + \Delta T)$ fitting provides the best fit to the experimental data although the temperature rise is small and consequently the A only model also fits the data reasonably well. The ΔT only model provides unphysical temperature changes of -20 K, and it is clear in this case that using a ΔT only model is unreasonable. The fitting results for the 610 cm^{-1} mode taken using the 514 nm laser are also summarized in Table 1.

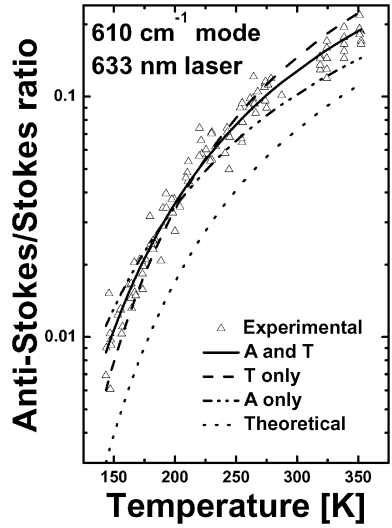

Fig. 2 Anti-Stokes/Stokes ratios as a function of temperature for the 610 cm^{-1} SERS active mode of RH6G using the 633 nm laser at low power. The solid line represents the fit to the experimental data using eqn. (2) whilst the dashed and dash dot lines represent the fits obtained from using only the ΔT or A parameter, respectively. The dotted line is the theoretical ratio values. See text for details.

4. Discussion and conclusions

In the results section we presented various types of fitting routines. For the experiments using the 514 nm laser it is clear that no significant heating takes place and fitting to a ΔT_{mode} only model is unphysical. The 633 nm data is more complex to interpret. For the lower energy modes the fitting is

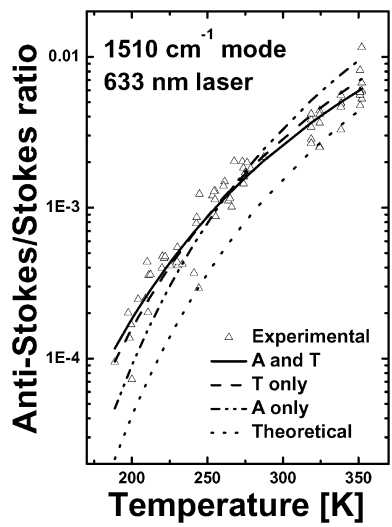

Fig. 3 Anti-Stokes/Stokes ratios as a function of temperature for the 1510 cm^{-1} SERS active modes of RH6G for the 633 nm laser at low power. This measurement is made over a smaller temperature range than that of the 610 cm^{-1} mode, which is shown in Fig. 2, because the intensity of the higher energy anti-Stokes mode decreases rapidly as a function of temperature. The solid line represents the fit to the experimental data using eqn. (2) whilst the dashed and dash dot represent the fits obtained from using only the ΔT or A parameter, respectively. The dotted line is the theoretical ratio values. See text for details.

Table 1 Fitting results for the 633 and 514 nm lasers both at low power, 0.5 mW, on large colloidal clusters using eqn. (2). Firstly there is the fitting with independent A's and ΔT shared among the modes. This is only possible for the 633 nm laser as only one mode is available for the 514 nm laser. Then there is the independent A's and ΔT fit or $(A + \Delta T)$ fit. Finally there is the A only and ΔT only fits for which only a single parameter was independently varied

	$A + \Delta T$ shared ($\Delta T = 25$ K)	$(A + \Delta T)$		A only	ΔT only
Mode	A	A	ΔT	A	ΔT
633 nm Laser					
610	1.31 ± 0.04	1.50 ± 0.05	17 ± 2	2.00 ± 0.04	39 ± 2
780	1.36 ± 0.05	1.63 ± 0.08	16 ± 2	2.33 ± 0.07	33 ± 2
1310	0.85 ± 0.04	0.47 ± 0.05	54 ± 5	1.6 ± 0.1	21 ± 2
1360	0.95 ± 0.04	0.8 ± 0.1	35 ± 5	1.9 ± 0.1	24 ± 1
1510	1.04 ± 0.05	0.7 ± 0.1	40 ± 4	2.2 ± 0.1	28 ± 1
514 nm Laser					
610	0.43 ± 0.02	3 ± 2		0.47 ± 0.01	−20 ± 1

ambiguous because a small temperature rise will not make such a significant difference to the population of excited states on the anti-Stokes side compared, for example, to higher energy modes. This is why fitting with the A only model describes the low mode data quite well. We also do not extract unphysical numbers when we fit to the ΔT only model as in the 514 nm case, suggestive that the scenarios are different for the two lasers. Finally fitting to the higher energy modes clearly shows that the $(A + \Delta T)$ fit routines work the best and that there is a definitive temperature rise. Mode specific heating is a rather an exotic effect and unlikely to be observable at low power so we can rule this out. Consequently although the data for the 610 cm^{-1} mode alone is not as clear-cut as that from the higher modes taken overall, there is clear evidence for a temperature rise using the 633 nm laser across all the modes.

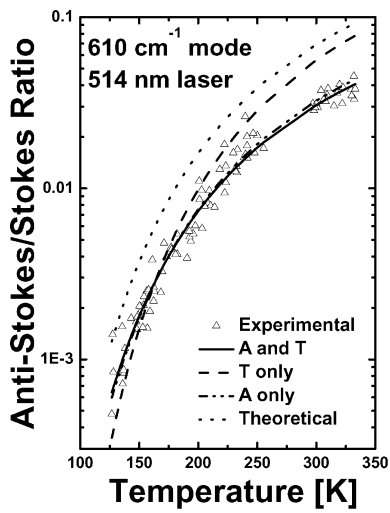

Fig. 4 Anti-Stokes/Stokes ratios as a function of temperature for the 610 cm^{-1} SERS active mode of RH6G for the 514 nm laser at low power. The solid line represents the fit to the experimental data using eqn. (2) whilst the dashed and dash dot lines represent the fits obtained from using only the ΔT or A parameter, respectively. The dotted line is the theoretical ratio values. See text for details.

There are four main observations which we can make from this work. In the first place by using a wide temperature range we are able to extract independent contributions from resonance effects (the A-factors in the fit) and increase of non equilibrium temperature (ΔT). Secondly, the fitting although open to some variability due to the scatter in the data has produced a rather systematic set of results. Thirdly, the pre-factor A mirrors the behavior that we have reported previously using 300 K only antiStokes–Stokes measurements. Namely that A decreases towards the critical value of one for higher energy modes for the 633 nm laser data and generally lies above the theoretical expectation and that A is typically smaller than one for the 514 nm laser data. These observations therefore rather robustly confirm the presence of a hidden resonance which peaks somewhere in the range between 514 nm and 633 nm. The final observation is that we find evidence for non equilibrium heating that is significant for the 633 nm laser and most clearly demonstrable for higher energy modes, as would be expected, because the relative change in intensity for a small temperature rise is larger for those. The fact that heating occurs with this laser and not with the 514 nm which is closer to the optical absorption peak of the dye again strongly supports our observations of a hidden resonance in this range. Previously we have attributed this resonance to a coupled dye–plasmon effect. Other explanations have been put forward in terms of a coupled plasmon resonance[12] which would, however, be highly geometry dependent.

In conclusion we have observed a laser frequency dependent heating of the order of 25 K at low laser power under SERS conditions with the 633 nm laser only. We attribute the heating to the rather narrow hidden resonance peak associated with the dye coupled plasmon. These observations have important implications for the use of SERS as an analytical method. The main result of this paper is that it is possible to a large extent to decouple the effect of thermal population and resonance contribution to the cross sections in the aS/S ratios by performing a wide temperature scan. This of course can only be performed for dried samples. The fact a simple model with only two parameters (asymmetry and heating parameter) can explain the data so well is remarkable in itself. This method, which has not been used for SERS in the past to the very best of our knowledge, extracts accordingly much more information on the physical conditions under which the SERS process is happening and overcomes the basic uncertainty in the different relative contributions to the aS/S ratios found at a single temperature.

Acknowledgements

PGE and LFC acknowledge partial support for this work by the Engineering and Physical Sciences Research Council (EPSRC) of the UK under grant GR/T06124. RCM acknowledges partial support from the National Physical Laboratory (NPL) in the UK.

References

1 M. Moskovits, *Rev. Mod. Phys*., 1985, **57**, 783.
2 A. Otto, in *Light Scattering in Solids*, ed. M. Cardona and G. Güntherodt, Springer, Berlin, 1984, p. 289.
3 K. Faulds, R. P. Barbagallo, J. T. Keer, W. E. Smith and D. Graham, *Analyst*, 2004, **129**(7), 567–568.
4 M. Green, F. M. Lui, L. Cohen, P. Kollensperger and A. Cass, in press.
5 J. J. Storhofff, R. Elghanian, C. A. Mirkin and R. L. Letsinger, *Langmuir*, 2002, **18**(17), 6666–6670.
6 J. Kneipp, H. Kneipp, W. L. Rice and K. Kneipp, *Anal. Chem*., 2005, **77**, 2381–2385.
7 C. Loo, A. Lowery, N. Halas, J. West and R. Drezek, *Nano Lett*., 2005, **5**(4), 709–711.
8 K. Kneipp, Y. Wang and H. Kneipp *et al*., *Phys. Rev. Lett*., 1996, **76**, 2444.
9 R. C. Maher, L. F. Cohen, P. Etchegoin, H. J. N. Hartigan, R. J. C. Brown and M. J. T. Milton, *J. Chem. Phys*., 2004, **120**, 11746.
10 T. L. Haslett, L. Tay and M. Moskovits, *J. Chem. Phys*., 2000, **113**, 1641.
11 A. G. Brolo, A. C. Sanderson and A. P. Smith, *Phys. Rev. B*, 2004, **69**, 45424.
12 R. C. Maher, J. Hou, L. F. Cohen, F. M. Liu, N. Green, R. J. C. Brown, M. J. T. Milton, E. C. Le Ru, J. M. Hadfield, J. E. Harvery and P. G. Etchegoin, *J. Chem. Phys*., accepted for publication.
13 E. C. Le Ru and P. G. Etchegoin, *Faraday Discuss*., 2006, **132**, DOI: 10.1039/b505343a.
14 K. Kneipp, H. Kneipp, I. Itzkan, R. R. Dasari and M. S. Feld, *J. Phys.: Condens. Matter*, 2002, **14**, R597.
15 H. Xu, J. Aizpurua, M. Käll and P. Apell, *Phys. Rev. E*, 2000, **62**, 4318.
16 P. C. Lee and D. Meisel, *J. Phys. Chem*., 1982, **86**, 3391.